Korean J. Chem. Eng., **30**(4), 937-948 (2013)
DOI: 10.1007/s11814-012-0221-y

Hydrogen recovery from Tehran refinery off-gas using pressure swing adsorption, gas absorption and membrane separation technologies: Simulation and economic evaluation

Ali Mivechian and Majid Pakizeh†

Department of Chemical Engineering, Faculty of Engineering, Ferdowsi University of Mashhad, P. O. Box 9177948974, Mashhad, Iran
(*Received 8 September 2012 • accepted 16 December 2012*)

Abstract−Hydrogen recovery from Tehran refinery off-gas was studied using simulation of PSA (pressure swing adsorption), gas absorption processes and modeling as well as simulation of polymeric membrane process. Simulation of PSA process resulted in a product with purity of 0.994 and recovery of 0.789. In this process, mole fraction profiles of all components along the adsorption bed were investigated. Furthermore, the effect of adsorption pressure on hydrogen recovery and purity was examined. By simulation of one-stage membrane process using co-current model, a hydrogen purity of 0.983 and recovery of 0.95 were obtained for stage cut of 0.7. Also, flow rates and mole fractions were investigated both in permeate and retentate. Then, effects of pressure ratio and membrane area on product purity and recovery were studied. In the simulation of the gas absorption process, gasoline was used as a solvent and product with hydrogen purity of 0.95 and recovery of 0.942 was obtained. Also, the effects of solvent flow rate, absorption temperature, and pressure on product purity and recovery were studied. Finally, these three processes were compared economically. The results showed that the PSA process with total cost of US$ 1.29 per 1 kg recovered H_2 is more economical than the other two processes (feed flow rate of 115.99 kmol/h with H_2 purity of 72.4 mol%).

Key words: Hydrogen Separation, PSA, Membrane, Gas Absorption, Off-gas

INTRODUCTION

Hydrogen is an important gas for producing clean and low sulfur fuels [1]. Due to new environmental regulations for production of sulfur-free fuels, hydrogen production in refineries and petrochemical plants has increased over the past years. In addition, more hydrogen is needed to enhance the capacity of hydroprocessing units plus high purity hydrogen, which is needed to increase the life of catalysts in these units [2]. A review of various uses of hydrogen in the industry was presented by Ramachandran and Menon [1]. Hydrogen gas is not found in nature in its pure form; therefore, investment in hydrogen production facilities is needed. Production of hydrogen from off-gas stream is one of the low-cost methods for hydrogen production [3]. In the past, refinery off-gas was transferred to refinery fuel gas system, in which only the thermal value of this stream was used. But nowadays, since hydrogen has become highly demanded in refineries, this stream has been considered as a source for hydrogen production. In addition, Hydrogen recovery from off-gas stream can reduce CO_2 emissions as a result of reducing the capacity of steam reforming unit [4].

In refineries, most of the make-up hydrogen is supplied from the catalytic reforming unit [5]. This unit is used to produce aromatic products and increase octane number of naphtha by dehydrogenation of the hydrocarbon molecules that results in the production of a large amount of hydrogen as a by-product stream, which is called catalytic reforming off-gas stream. In Tehran Refinery, a part of this stream is sent to the refinery fuel system. Because there is a considerable amount of hydrogen in this stream, it would be economical to build a unit for recovering hydrogen and supply hydrogen to the other processing units. The hydrogen recovery unit that produces hydrogen from the reactor exhaust gas of catalytic reforming produces two gas streams, pure hydrogen and tail-gas stream. The tail-gas stream includes C_1-C_6^+ and can be sent to the refinery fuel gas system if needed. Also, purified hydrogen can be fed into the second stage of the make-up hydrogen compressor. The recovered hydrogen can be combined with the make-up hydrogen to bring the purity to 0.94-0.96 [6]. Methane is the major impurity in the catalytic reforming off-gas stream and is difcult to remove, entering methane to the hydroprocessing unit can cause catalyst deactivation through coke formation, and therefore it must be removed before entering this unit [6]. The three common methods that are used for hydrogen purification are PSA, polymeric membrane and gas absorption processes.

Some researchers have studied these processes. Mehra and Al-Abdulal [7] introduced gas absorption process for hydrogen recovery. They specified a range for gas absorption process; a feed stream with 0.50 to 0.90 hydrogen content could be purified to 0.9-0.98. Peramanu et al. [8] investigated different processes to find the best suitable process for hydrogen recovery in several case studies. They studied gas absorption with iso-octane solvent and reported that hydrogen with purity of 0.805 and recovery of 0.957 was produced from high pressure off-gas stream with hydrogen purity of 0.736. Al-Rabiah [9] studied hydrogen separation in an ethylene plant by two-stage membrane system that produced purified hydrogen stream with purity of 0.98 and recovery of 0.92 from a feed stream with

†To whom correspondence should be addressed.
E-mail: pakizeh@um.ac.ir

0.192 hydrogen purity. Kaldis et al. [10] indicated that even for a one-stage membrane unit, high hydrogen permeate purity (up to +0.99) and signicant total recovery (up to 0.90) can be achieved for moderate to high (0.2-0.6) stage cuts. Also, several studies have been conducted on PSA process for hydrogen purification [11-13]. These studies have indicated that product with very high hydrogen purity (+0.99) and recovery of 0.65-0.85 depending on adsorption pressure, can be obtained using the PSA process.

In the present work, simulation of PSA, membrane and gas absorption technologies for hydrogen recovery from Tehran refinery off-gas has been performed. In the PSA process, silica gel (for removing C_4^+) and activated carbon (for removing C_1-C_3) were used as adsorbents, and effect of adsorption pressure on the product purity and recovery was studied. In the membrane process, effects of membrane area, and feed and permeate pressure on hydrogen purity and recovery of product were studied. Also, as a new approach, simulation of gas absorption process for hydrogen recovery was conducted under temperature below 0 °C. This temperature was provided by propane refrigerator. Then, effects of absorption temperature and pressure and solvent flow rate were investigated on hydrogen purity and recovery of product in gas absorption process. Finally, economic evaluation and sensitivity analysis of these three processes were investigated and compared.

SEPARATION TECHNOLOGIES

1. Pressure Swing Adsorption

The separation process using PSA is based on adsorption and is used for purification of gases like hydrogen in refineries. Depending on the process, adsorbents like molecular sieve, activated carbon, and silica gel are used in PSA beds. For the recovery of hydrogen from off-gas stream, activated carbon and silica gel are used most of the time. PSA is able to produce nearly pure hydrogen. In the PSA process, gases C_1, C_2, C_3, and heavier hydrocarbons are adsorbed by the adsorbent and pure hydrogen is obtained. Gas adsorption is strongly dependent on pressure. With increasing pressure, the adsorption capacity of adsorbents rises and vice versa. In the PSA unit pressure drop is low, so product pressure is near feed pressure. On the other hand, tail-gas pressure is low, because process swings to low pressure to desorb the impurities from the adsorbents. To have a continuous pure product flow, as soon as the adsorbents reach maximum capacity, feed should be fed to the other bed which is regenerated from impurities. At the same time, the saturated bed must be desorbed and made ready for the next step. Usually, several beds are needed in process for production of purified hydrogen; while one of them is producing high purity product, other beds are being regenerated at the same time. The PSA process is simple, but its design is complex. Some important benefits of using the adsorption process are utilizing sour gas and water separation capability simultaneously.

2. Polymeric Membrane

Hydrogen recovery using polymeric membrane is based on differences between permeability of feed stream components. Gases with high permeability pass through the membrane faster than the other gases. In this process, hydrogen is more permeable than methane and heavier hydrocarbons and passes through the membrane faster. So, the product stream will be enriched in hydrogen. Higher hydrogen permeability leads to better separation and lesser required energy for the process. Product purity is strongly influenced by membrane selectivity and the pressure difference between feed and permeate. To enhance hydrogen recovery, membrane area should be increased. Another way to reach higher recovery is increasing pressure difference between the two sides of the membrane, which can impose additional costs in order to raise the pressure of feed or product stream. The membranes usually need to be replaced every 4 to 5 years due to loss of performance.

Off-gas stream, which is generated in Tehran refinery, has a dew point of about 34 °C and includes hydrogen at 72%; methane, ethane, and propane add up to 25%, and heavier hydrocarbons at 3%. Because the dew point of retentate rises above the off-gas stream temperature, removal of hydrogen through the membrane can cause condensation of heavy compounds within the membrane. If polymeric membrane is in contact with liquid hydrocarbon, the membrane will be damaged [4,14]. Therefore, to avoid condensation of heavy hydrocarbons in the membrane, the off-gas stream should be heated to the dew point of retentate stream (75 °C). But in terms of operation, for optimal separation, the feed should be heated 15-20 °C higher than this temperature [14].

3. Gas Absorption

Gas absorption by liquid solvent is one of the oldest and most well-known separation processes in refineries that can be used to purify gas streams. Absorption of light hydrocarbons from a hydrogen stream into a hydrocarbon solvent is called the sponge oil process [8]. This process is based on the solubility of hydrocarbons in the solvent. A good candidate solvent for this process should not only remove the maximum amount of impurities and the minimum amount of hydrogen, but also should be easily regenerated from the absorbed impurities. The solvent can be supplied from the existing refinery streams, which has been considered gasoline in this paper. Effects of different solvents on this process were studied experimentally by Peramanu [15]. In this process, pure hydrogen is produced as a result of passing the feed stream through the absorption tower in which impurities are absorbed by solvent at feed pressure and at temperature below 0 °C. The solvent is regenerated by decreasing pressure in some consecutive steps and then is returned to the tower. Because the pressure of hydrogen that leaves the process is near feed pressure, the costs of increasing product pressure for entering into the second stage of the make-up compressor aren't considerable. It should be noted that in this process recovery is not 100 percent: a little bit of hydrogen gas is absorbed by the solvent and exited from system with the mixture of hydrocarbons. One advantage of this process is that the liquid solvent has the capability of separating hydrogen sulfide in addition to the other impurities.

SIMULATION

1. Pressure Swing Adsorption

Simulation of the process is performed using the Aspen Adsorption simulator. The following assumptions were made for developing the simulation:

- Peng-Robinson equation of state is applied for thermodynamic calculation.
- Isothermal Energy balance.
- The flow pattern is described by the axially dispersed plug flow

Table 1. The characteristics of the adsorption bed and adsorbents [11,16]

Adsorption bed	
Length	5.5 m
Internal diameter	1 m
Bed void fraction	0.4
Adsorbent	Silica gel
Length	1.75 m
Particle size	2.36 mm
Particle porosity	0.44
Apparent density	1.15 gr cm^{-3}
Adsorbent	Activated carbon
Length	3.75 m
Particle size	2.36 mm
Particle porosity	0.58
Apparent density	0.87 gr cm^{-3}

model.

- Adsorbents: silica gel and activated carbon.
- Hydrogen is almost inert to silica gel.

The characteristics of the adsorption bed and adsorbents are given in Table 1. Langmuir isotherm equation was used for observing adsorption of multicomponent mixture on adsorbents which is as follows:

$$q_i = \frac{q_{mi} b_i P_i}{1 + \sum_j b_j P_j} \qquad , j=1, 2, 3, \ldots, m \tag{1}$$

$$b_i = b_{0i} \exp\left(\frac{-\Delta H_{Ai}}{RT}\right) \tag{2}$$

Where q_i is the equilibrium loading of component i, P_i is the partial pressure of component i, T is the temperature, and q_{mi}, b_{0i}, $(-\Delta H_{Ai})$, are the isotherm parameters. The isotherm parameters for hydrocarbons are given in Table 2 [11,16]. To investigate behavior of C_5 and C_6 in silica gel and activated carbon, isotherm parameters of butane were used. Also, the hydrogen adsorption isotherm model for activated carbon is linear [11]. This isotherm equation is as follows:

Table 2. Langmuir isotherm parameters [11,16]

Silica gel			
	q_{mi}	b_{0i}	$-\Delta H_{Ai}$
Methane	1.76	5.05E-04	1.28E+04
Ethane	1.611	2.34E-05	2.56E+04
Propane	3.765	1.84E-04	2.01E+04
Butane	2.344	1.59E-05	3.10E+04
Activated carbon			
	q_{mi}	b_{0i}	$-\Delta H_{Ai}$
Methane	5.8243	1.92E-04	1.66E+04
Ethane	5.4738	5.61E-05	2.51E+04
Propane	3.7348	4.11E-04	2.64E+04
Butane	3.635	5.57E-07	4.44E+04

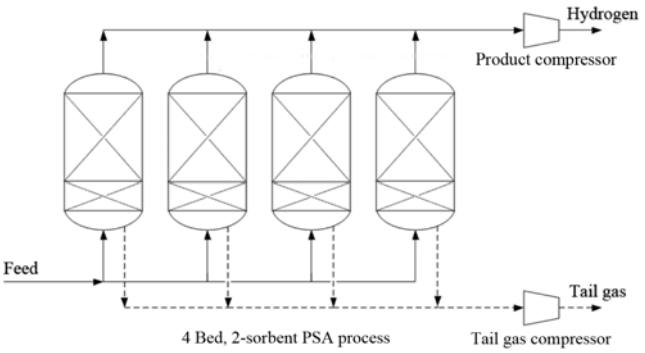

Fig. 1. Diagram of PSA process for hydrogen recovery.

$$q_{H_2} = 0.00769 \exp\left(\frac{624.25}{T}\right) P_{H_2} \tag{3}$$

The diagram of process is shown in Fig. 1. Because the pressure of recovered hydrogen is near feed pressure, it should be compressed to 31.63 bar and then fed into the second stage of the make-up compressor. Tail-gas can also be compressed and then transferred to the refinery fuel gas system.

2. Polymeric Membrane

Modeling and simulation of the membrane separation process was performed using Aspen Custom Modeler (ACM) simulator. Assumptions made for simulating hydrogen recovery using membrane process are as follows:

- Separation is based on the solution-diffusion model.
- Retentate pressure is considered equal to feed pressure.
- Permeate and retentate pressures are fixed.
- Temperature is constant.

Base of modeling is shown in Fig. 2. Membrane module is divided into n equal small segments in which governing equations on each segment k are as follows:

$$F_R^{k-1} = F_R^k + F_{P,1}^k \tag{4}$$

$$F_{P,1}^k \cdot y_{i,1}^k = A_S \cdot Q_i \cdot (P_R \cdot x_i^k - P_P \cdot y_{i,1}^k) \tag{5}$$

$$F_R^{k-1} \cdot x_i^{k-1} = F_R^k \cdot x_i^k + F_{P,1}^k \cdot y_{i,1}^k \tag{6}$$

In Eq. (5), Q_i is the permeance of component i, A_S is the area available for mass transfer in each segment, and P_R, and P_P, are the retentate and permeate pressures. This equation is obtained by performing the mass conservation over A_S for a multicomponent gas mixture

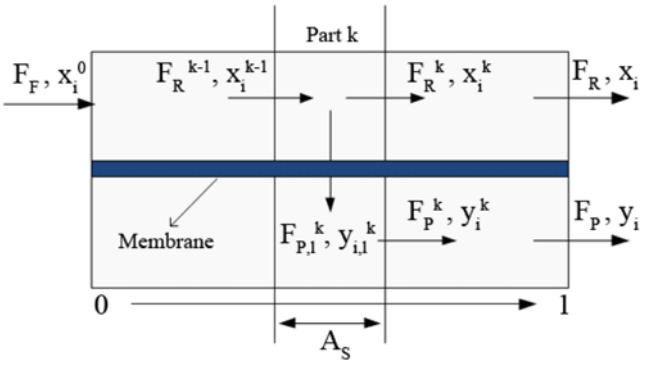

Fig. 2. Schematic of the flows and mole fractions of component i in the membrane system.

[17].

In each segment and for each component we have:

$$\sum x_j^k = 1 \qquad , j=1, 2, \ldots, m \tag{7}$$

By numerically solving these equations simultaneously in a cocurrent flow pattern for segment k, the $\mathbf{F}_{P,I}^k$ and $\mathbf{y}_{i,I}^k$ that entering permeate side and the $\mathbf{F}_R^k$ and $\mathbf{x}_i^k$ that entering segment k+1 are obtained. First, the equations are solved for the first segment of the module. Then, the results are used for solving the next segment's equations. This procedure goes on until the end of the membrane module, where the permeate and retentate exit at n^{th} segment. It is clear that $\mathbf{F}_R = \mathbf{F}_R''$ and $\mathbf{x}_i = \mathbf{x}_i''$. To obtain $\mathbf{F}_P^k$ and $\mathbf{y}_i^k$ for component i, Eq. (8) and Eq. (9) have to be solved simultaneously over k successive segments which stretch from the module input to the distance z. Flow rate and composition of permeate exiting from membrane module are obtained by solving Eq. (8) and Eq. (9) over the entire membrane (k=n, z=L, $\mathbf{F}_P = \mathbf{F}_P''$, $\mathbf{y}_i = \mathbf{y}_i''$).

$$F_P = \sum F_j^P \qquad , j=1, 2, \ldots, k \tag{8}$$

$$F_F \cdot x_i^0 = F_R^k \cdot x_i^k + F_P^k \cdot y_i^k \tag{9}$$

Polyimide membrane with hydrogen permeance of 500 GPU† was chosen for simulation in which selectivity of hydrogen over methane (H_2/C_1) and other components (H_2/C_2^+) was 125 and 590, respectively [9]. In this case, hydrogen passes through the membrane faster than hydrocarbons due to high selectivity, so the permeate stream will be enriched in hydrogen.

Kaldis et al. [10] studied hydrogen separation using polyimide membrane for six different feed conditions (a)-(f). Fig. 3 and Fig. 4 represent their results. These results were used to validate our membrane model in the present work. For this purpose a feed stream with 0.799 hydrogen content, (f), was considered (25 bar, 2,315 Nm^3/h). Fig. 5 shows the results of our membrane model in the present work for (f) stream which must be compared with (f) curve on Fig. 3 and Fig. 4. Our results in Fig. 5 are similar to the reported results by Kaldis et al. [10] which are shown in Figs. 3 and 4.

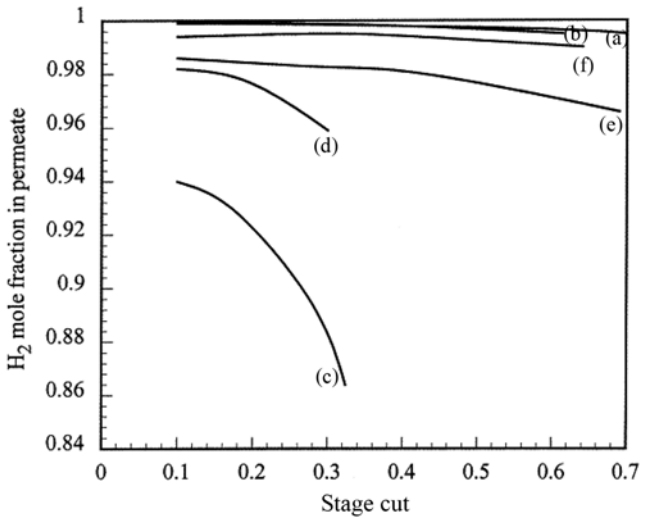

Fig. 3. Effect of stage cut on hydrogen permeate mole fraction reported by Kaldis et al. [10]. Feed stream of (f) is considered in present study to validate our membrane model.

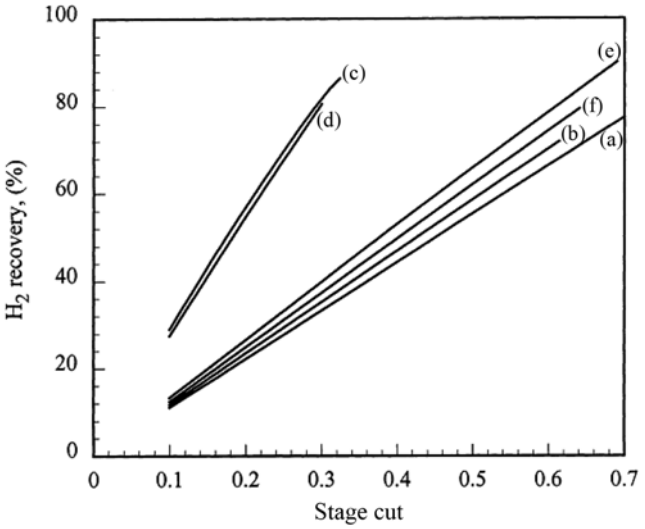

Fig. 4. Effect of stage cut on hydrogen recovery reported by Kaldis et al. [10]. Feed stream of (f) is considered in present study to validate our membrane model.

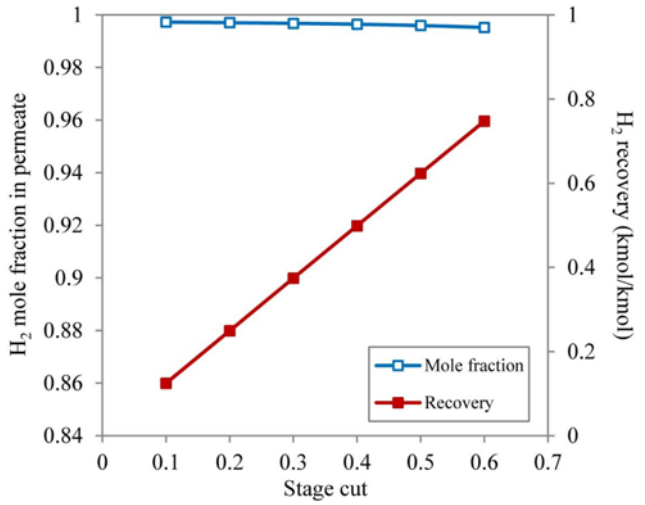

Fig. 5. Results of our membrane model for feed stream of (f).

The diagram of membrane separation process for hydrogen recovery is shown in Fig. 6. Pressure in the permeate side, is markedly lower than feed pressure, so hydrogen product should be compressed in two steps and then can be fed into second stage of the make-up compressor.

3. Gas Absorption

Simulation of gas absorption process has been done by using the Aspen HYSYS simulator. NRTL model was used to develop the simulation. The separation is based on purification of hydrogen by absorbing hydrocarbons into liquid solvent, at temperature below 0 °C. This low temperature is provided by a refrigerator stream which is in a cycle.

Gasoline was used as the solvent in this simulation. The composition of this gasoline is shown in Table 3 [18]. A diagram of the simulated process is depicted in Fig. 7. Feed and solvent streams are cooled below 0 °C by two heat exchangers of E-101 and E-102, respectively, and then are fed into the absorption tower.

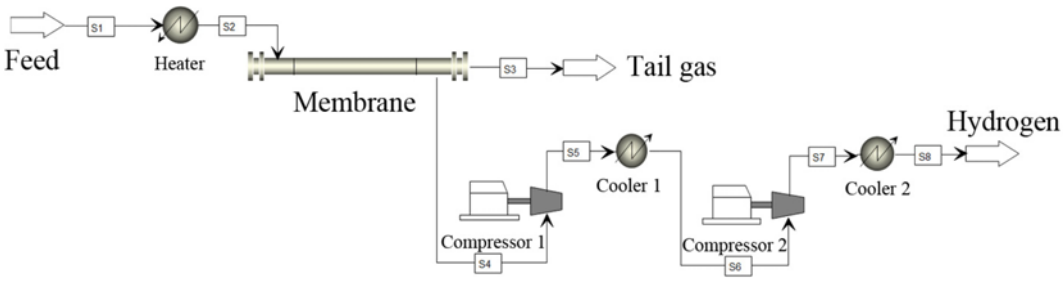

Fig. 6. Flow diagram of one-stage membrane process for hydrogen recovery.

Table 3. Composition of gasoline used as solvent in simulation [18]

Component	Mole fraction
n-Pentane	0.00906
Cyclopentane	0.00942
2-Methyl pentane	0.16483
3-Methyl pentane	0.11311
Methyl cyclopentane	0.04515
Cyclohexane	0.02944
n-Hexane	0.2857
3-Methyl hexane	0.0577
2-Methyl hexane	0.05111
n-Heptane	0.13519
n-Octane	0.06508
n-Decane	0.02786
n-Undecane	0.00634

Solvent regeneration occurs in the three stage pressure reduction, and then the solvent is returned into the absorption tower, after its pressure is increased by the pump.

RESULTS AND DISCUSSION

1. Pressure Swing Adsorption

The performance of a PSA system with a 5.5 m height bed containing 1.75 m silica gel and 3.75 m activated carbon as adsorbents was simulated in which the bed diameter was assumed 1 m. Specification of feed stream is given in Table 4. Simulation results showed that PSA process product is a hydrogen stream with recovery of 0.789 and purity of 0.994. Figs. 8 to 10 show mole fraction profiles of the components in the bed. The first part of the bed is filled with silica gel and the second part of that with activated carbon, so in Fig. 8 to Fig. 10, the x-axis from 0 to 1.75 m and after 1.75 m represents the profiles of the components in silica gel and activated carbon parts of the bed, respectively. In these figures, the profiles of the components are represented at 4 and 7 minutes after starting the adsorption process. Hydrogen mole fraction profiles in the bed during the adsorption time are shown in Fig. 8. With increasing adsorption of impurities, the hydrogen purity increases. As illustrated

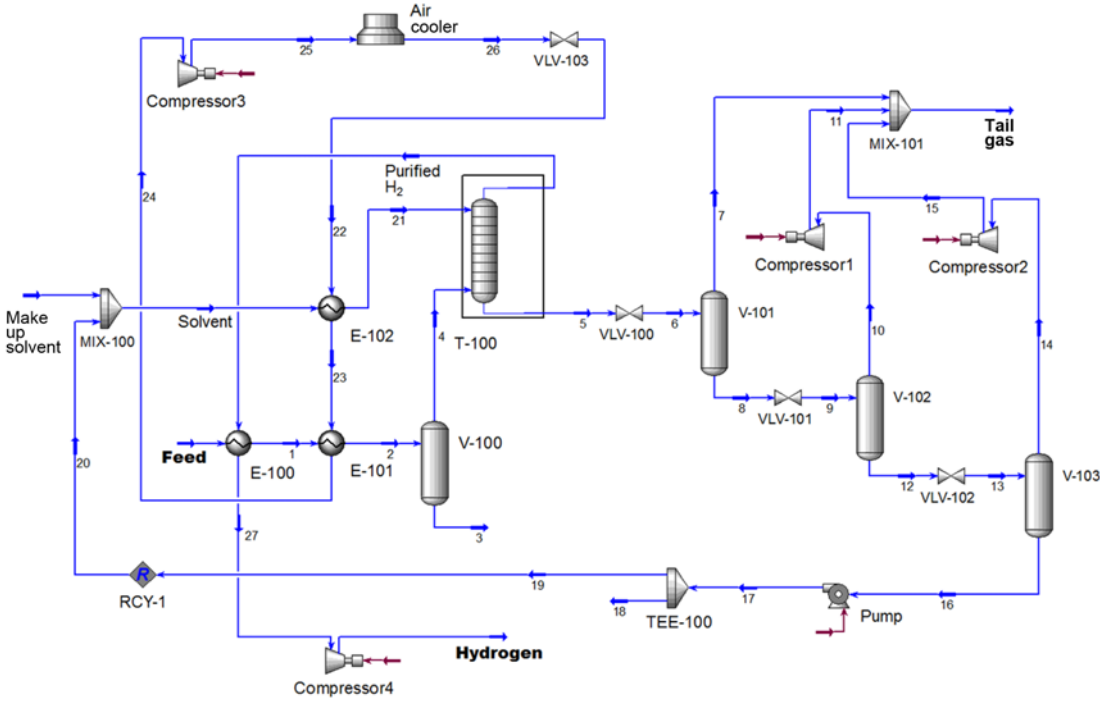

Fig. 7. Flow diagram of gas absorption process for hydrogen recovery.

Table 4. The specification of feed stream

Flow rate, kmol/h	115.99
Pressure, bar	24.13
Temperature, C	37.7
Mole fraction	
H_2	0.724
C_1	0.119
C_2	0.080
C_3	0.044
C_4	0.020
C_5	0.007
C_6	0.006

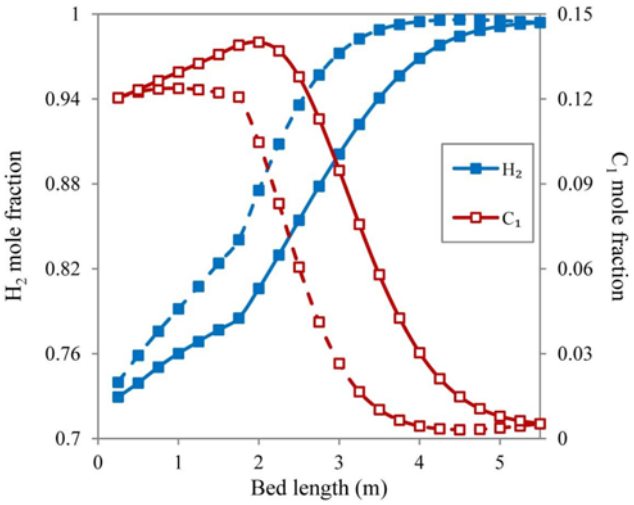

Fig. 8. Mole fraction profiles of hydrogen and methane along bed length. Dashed and solid lines represent the mole fraction profiles at time of 4 min and 7 min, respectively.

in Fig. 8, at the adsorption process, over time, initial adsorption capacity of the adsorbents begins to fall. This leads to the removal of impurities, and the maximum hydrogen purity is met at the higher part of the bed. According to Fig. 8, if the adsorption time becomes longer than 7 minutes, the purity of the output product is reduced. In this case, the feed can be redirected to the next bed to prevent reduction in the product purity.

Also, Fig. 8 shows that the methane mole fraction profile is changed in the bed length during the adsorption step. It could be concluded from Fig. 8 that during the adsorption time, that lasts 7 minutes, methane is adsorbed and its content gradually is reduced to near zero. With reduction in the adsorption capacity of the adsorbents over time, methane content reduction to near zero takes place in a higher part of the bed. Also, from the methane profile in the bed, the purity of methane is increased, reaches a peak and then falls rapidly. The primary growth is due to the elimination and reduction of the purity of lighter compounds.

Ethane and propane mole fraction profiles along the bed length over 7 minutes of adsorption process are shown in Fig. 9. As can be seen, ethane and propane are being removed along the bed length like methane, but because of the higher adsorption ability of ethane and propane in comparison with methane, and also their lower purity,

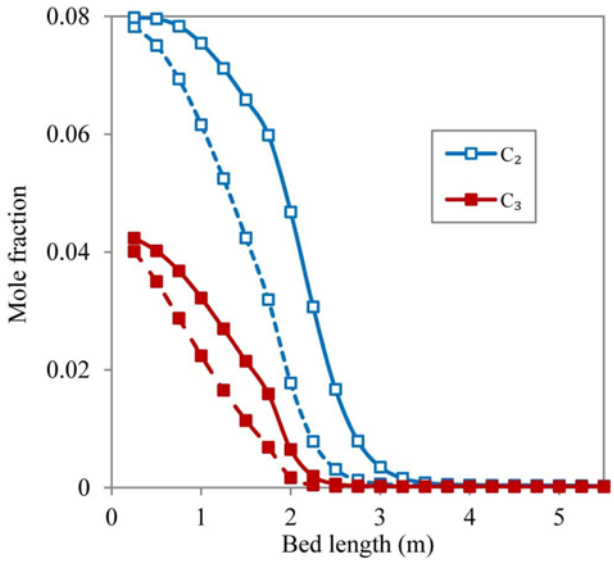

Fig. 9. Mole fraction profiles of ethane and propane along bed length. Dashed and solid lines represent the mole fraction profiles at time of 4 min and 7 min, respectively.

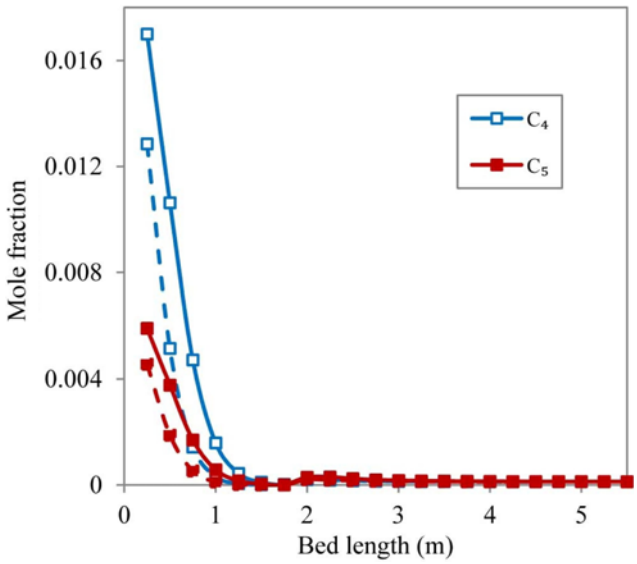

Fig. 10. Mole fraction profiles of butane and pentane along bed length. Dashed and solid lines represent the mole fraction profiles at time of 4 min and 7 min, respectively.

these components are almost totally removed in the early part of activated carbon adsorbent.

The heavier compounds, C_4^+, could be adsorbed by both adsorbents, silica gel and activated carbon; since the desorption of heavy compounds from activated carbon is harder than silica gel, silica gel is used as the first adsorbent in the bed most of the time. Butane and pentane mole fraction distribution along the bed are shown at two different time points in Fig. 10. As can be seen, these components are almost totally removed by silica gel adsorbent in the bed. Hexane's profile is not shown in Fig. 10, but this curve almost coincides with the pentane curve. In Fig. 10, there is an increase in mole fraction after silica gel part of bed. This increase is a negligible simulation error which can be ignored.

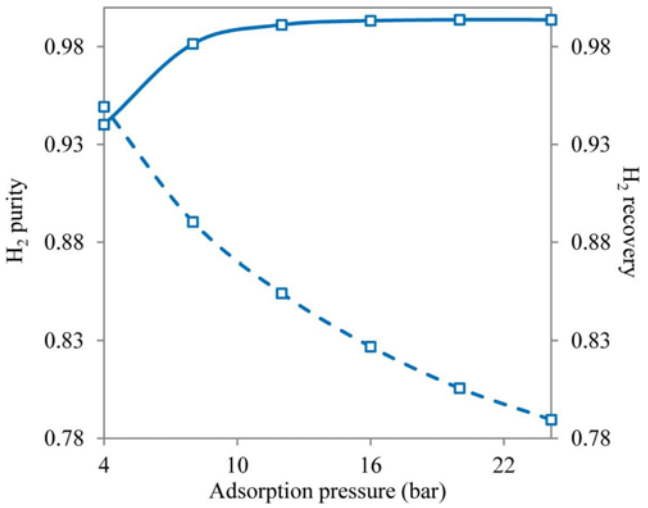

Fig. 11. Effect of adsorption pressure on hydrogen purity and recovery. Solid line represents the purity (left y-axis) and dashed line represents the recovery (right y-axis).

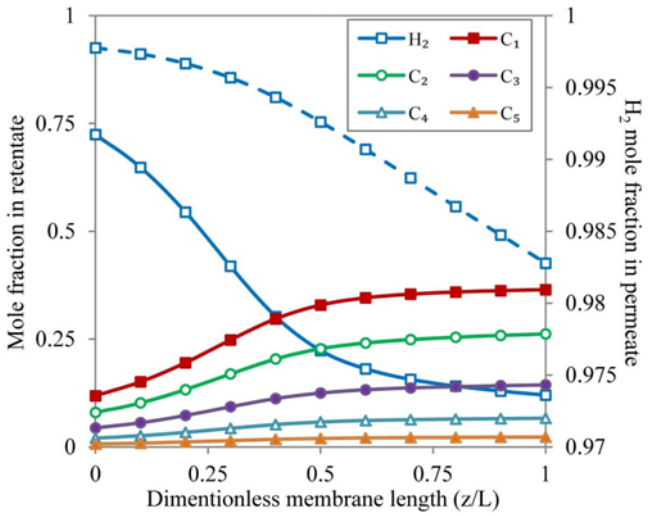

Fig. 13. Hydrogen and other component mole fraction profiles along membrane. Solid lines represent the profiles of components in retentate side and are scaled on the left y-axis. Dashed line represents the profile of H_2 in permeate side and is scaled on the right y-axis.

Fig. 11 shows recovery and purity of hydrogen product versus feed pressure. This figure illustrates that with decreasing feed pressure, the purity is decreased and the recovery is enhanced. Reducing pressure under the fixed system configuration decreases adsorption of gases. Consequently, more hydrogen and impurities exit as product stream, which leads to hydrogen purity reduction and recovery enhancement.

2. Polymeric Membrane

Polyimide membrane with a surface area of 334 m^2 was used for simulation. Feed flow rate of 115.99 kmol/h at pressure of 24.13 bar entered the module, and purified hydrogen at pressure of 4 bar was obtained. The simulation resulted in hydrogen with purity of 0.983 and recovery of 0.95.

The membrane area in the direction of the feed stream was divided into 100 equal parts; profiles of flow rates and mole fractions versus the membrane length are depicted in Fig. 12 and Fig. 13. Membrane length was normalized between 0 and 1, so 0 represents the feed input point of the membrane module and 1 represents membrane output where retentate and permeate streams have exited. The profiles of permeate and retentate flow rate versus membrane length are depicted in Fig. 12. The results show that permeate and retentate flow rate from the membrane module was 81.22 kmol/h and 34.77 kmol/h, respectively.

Fig. 13 shows the hydrogen purity versus the membrane length in permeate side. It is clear from this figure that permeate has left

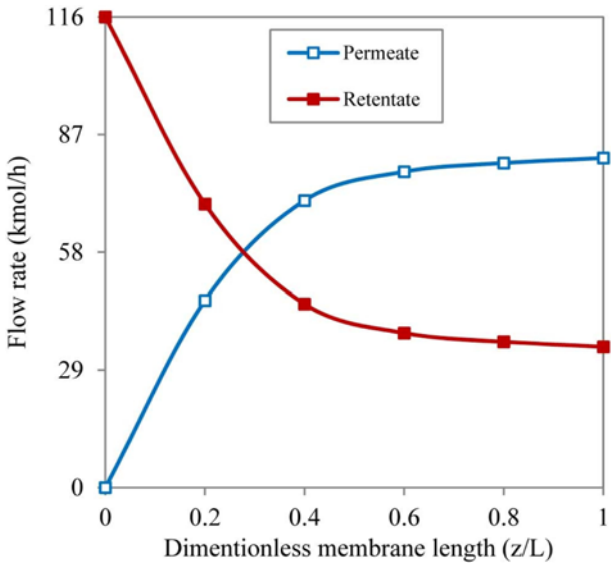

Fig. 12. Flow rates of permeate and retentate along membrane length.

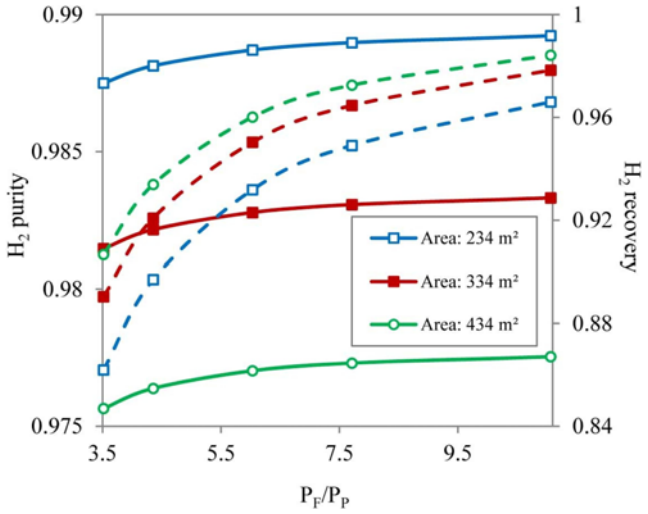

Fig. 14. Effects of pressure ratio and membrane area on hydrogen purity and recovery. Solid lines represent the purity and are scaled on the left y-axis. Dashed lines represent the recovery and are scaled on the right y-axis. The pressure difference between the feed and permeate pressure (P_F-P_P) is maintained constant at 20 bar.

the membrane module with hydrogen purity of 0.983. As we move along the membrane, the purity of hydrogen in permeate side slightly is reduced, as a consequence of steep reduction in hydrogen purity at retentate side.

Profiles of mole fractions of hydrogen and other components versus membrane length in retentate side are shown in Fig. 13. As can be seen, the purity of hydrogen was reduced, but the purity of other compounds was increased in retentate. At the end, the retentate has left the membrane module with hydrogen purity of 0.12. The hexane curve is not shown in the Fig. 13, but this curve almost coincides with the pentane curve.

The effects of pressure ratio (the ratio of feed to permeate) and membrane area on the purity and the recovery of product are shown in Fig. 14. Increasing the pressure ratio increases hydrogen purity and recovery. Increasing pressure ratio increases permeate flow rate due to increasing overall driving force across the membrane, which leads to hydrogen purity and recovery enhancement. By increasing the membrane area, the purity was decreased but the recovery was increased. Increasing membrane area increases permeation of both hydrogen and impurities cross the membrane. Consequently, increasing permeation of hydrogen increases hydrogen recovery in permeate side. The rate of increasing permeation as a function of area in impurities is higher than that in hydrogen, which results in reduction of hydrogen purity.

3. Gas Absorption

In the gas absorption process, feed temperature was decreased to −18 °C and flow rate of solvent set to be 480 kmol/h. Simulation results indicate that gas absorption provides a hydrogen purity of 0.95 and recovery of 0.942 from the off-gas stream.

Mole fraction profiles of the three lighter components, in the gas stream, along the absorption tower are presented in Fig. 15. The methane mole fraction starts to fall gradually and continues to decrease more steeply at higher tray positions. In contrast, ethane mole fraction decreases rapidly and then levels off gradually. Also, the hydrocarbons which are heavier than ethane have the same behavior. In the early part of the tower, the rate of removing C_2^+ hydrocarbons is more than C_1 due to higher solubility and selectivity. Absorption rate of methane significantly increased, after a significant amount of C_2^+ hydrocarbons were removed.

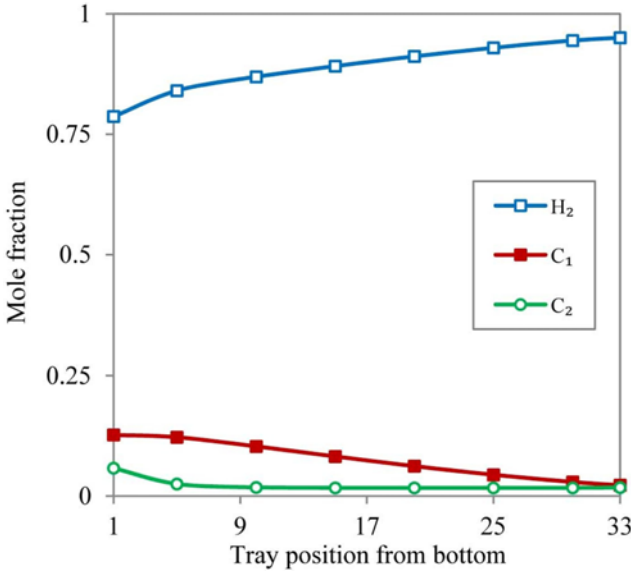

Fig. 15. Mole fraction profiles of hydrogen, methane and ethane along absorption tower.

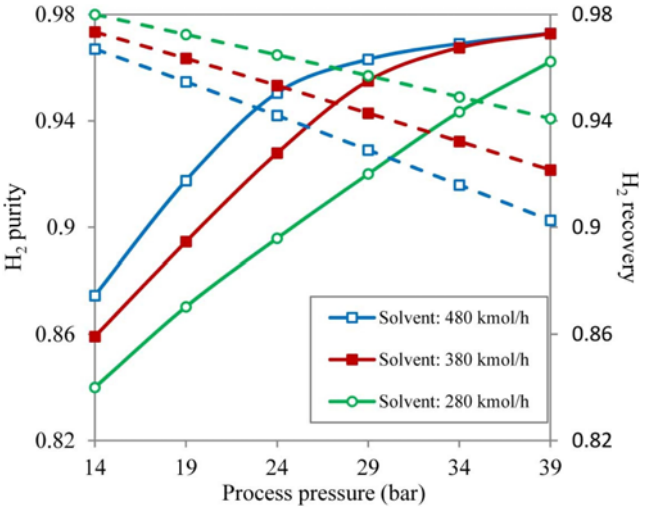

Fig. 16. Effects of process pressure and solvent flow rate on hydrogen purity and recovery. Solid lines represent the purity and are scaled on the left y-axis. Dashed lines represent the recovery and are scaled on the right y-axis.

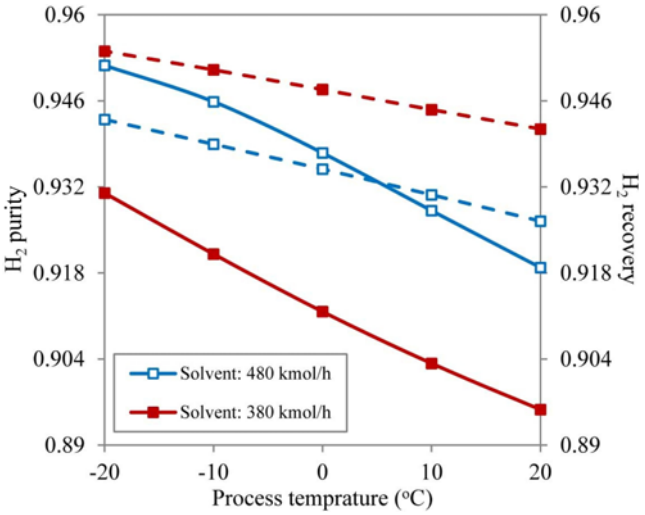

Fig. 17. Effects of process temperature and solvent flow rate on hydrogen purity and recovery. Solid lines represent the purity and are scaled on the left y-axis. Dashed lines represent the recovery and are scaled on the right y-axis.

Since tower pressure and temperature and solvent flow rate are effective factors in the product recovery and purity of the gas absorption process, the influences of these parameters on hydrogen recovery and purity have been investigated in Fig. 16 and Fig. 17. From Fig. 16, it is observed that hydrogen purity is increased by increasing pressure. Also, increasing the flow rate of solvent has a direct impact on the purity of the product. Fig. 16 shows that increasing the pressure and solvent flow rate decreases recovery. Increasing pressure and solvent flow rate leads to increase in absorption of hydrogen and impurities by solvent. Absorption of more im-

Table 5. Material balance of hydrogen recovery from Tehran refinery off-gas

	Units	PSA	Membrane	Gas absorption
Feed				
Flow rate	kmol/h	115.99	115.99	115.99
Pressure	bar	24.13	24.13	24.13
H_2 purity	kmol/kmol	0.724	0.724	0.724
Output streams				
H_2 recovery	kmol/kmol	0.789	0.950	0.942
Product rate	kmol/h	66.72	81.22	83.23
Product pressure	bar	31.63	31.63	31.63
Product H_2 purity	kmol/kmol	0.994	0.983	0.950
Tail gas rate	kmol/h	49.27	34.77	27.07
Tail gas pressure	bar	4	24.13	4
Tail gas H_2 purity	kmol/kmol	0.359	0.120	0.178
Electric power				
Product compressor(s)	kW	20.9	209.6	19.5
Tail gas compressor(s)	kW	50.3	-	17.1
Refrigerator compressor	kW	-	-	355.6
Cooling water				
Product coolers	m^2/h	-	1.016	-
Steam				
Feed heater	kg/h	-	1,950	-

purities increases hydrogen purity of the gas stream; on the other hand, absorption of more hydrogen reduces recovery of purified hydrogen.

If the concentration of impurities is sufficiently low, it is difficult to remove them by increasing solvent flow rate. Consequently, if the pressure is sufficiently high, there is a specified amount of solvent flow rate at which increasing more solvent flow rate does not increase purity significantly, but decreases recovery obviously. For example, as can be seen in Fig. 16, the process gives similar hydrogen purity for both 380 and 480 kmol/h solvent at pressure of 34 bar. But, as Fig. 16, using 380 kmol/h solvent gives higher hydrogen recovery. So, increasing the solvent flow rate more than 380 kmol/h isn't beneficial at pressure of 34 bar.

Also, effects of the tower temperature and solvent flow rate on product purity and recovery were investigated in Fig. 17. As can be seen, decreasing temperature increases hydrogen purity and recovery. Reducing temperature decreases the absorption of hydrogen due to reduction of its solubility and consequently increases hydrogen recovery. In contrast, more impurities are absorbed by solvent, which results in hydrogen purity enhancement.

ECONOMIC COMPARISON

PSA, polyimide membrane, and gas absorption processes with hydrogen product purity of 0.994, 0.983, and 0.95 and recovery of 0.789, 0.95, and 0.942, respectively, for hydrogen recovery from Tehran refinery off-gas were economically compared. The economic calculations were done based on the equipment shown in Figs. 1, 6 and 7. All equipment costs were estimated using cost estimation methods which are represented by Seider and Seader [19]. These costs were calculated in 2011 USD. In this study we assumed an annual interest rate of 12.5% and a depreciation time of 10 years. CAPEX (capital expenditure) was based on direct and indirect cost. Direct costs include equipment cost, installation cost, piping, electrical system, building, etc. Indirect costs include engineering and supervision, contractor's fee, contingency, etc. OPEX (operating expenditure) was based on utilities, operating labor, maintenance and repairs, etc. Hydrogen recovery from off-gas stream reduces the amount of feed that is delivered to the refinery fuel system. As a result, the amount of produced energy in the refinery fuel system is decreased substantially. Natural gas was used to offset the amount of this energy. The cost of supplying a refinery fuel system with natural gas is called the lost fuel gas cost, which was considered in economic evaluation. Table 5 shows the material balance for each process, and the cost sheet of these processes is given in Table 6. It is clear from Fig. 18 that PSA is more economical than the other processes. As can be seen, the cost of recovering 1 kg hydrogen using the PSA, the membrane and the gas adsorption processes, was calculated to be US$ 1.29, 1.39 and 2.32, respectively.

According to Table 6, each of the CAPEX, OPEX and lost fuel gas cost for PSA process were lower than for the membrane and gas absorption processes. Most of the total equipment cost and the utility cost for the gas absorption process was related to the compressor in the refrigeration cycle and for membrane process was related to increasing product pressure. In PSA, the total cost of compressors was very low in comparison to the other two processes.

Sensitivity analysis of the feed flow rate on economics of different processes is shown in Fig. 19. The effect of increasing the feed flow rate to 1.5F and 2F (F=115.99 kmol/h) on economics of each process was investigated. Increasing feed flow rate decreased cost of producing 1 kg H_2 in the three processes. On the other hand, by increasing feed flow rate, the total cost ratio of PSA to membrane or gas absorption processes became lower. For example, at flow rate of F, total cost ratio of PSA to gas absorption was 0.55; this

Table 6. Cost sheet of hydrogen recovery from Tehran refinery off-gas

	Basis	PSA	Membrane	Gas absorption
Capital expenditure (US$)				
Product compressor(s)		200,688	1,501,076	190,383
Tail gas compressor(s)		405,191	-	195,418
Refrigerator compressor		-	-	1,938,585
Non- compressor equipment		1,444,707	578,963	3,819,023
Sub-total		2,050,585	2,080,039	6,143,409
Operating expenditure (US$/y)				
Steam	$5.5/1,000 kg	-	90,090	-
Cooling water	$0.013/m^3	-	111	-
Electricity	$0.07/kW·hr	41,826	123,245	260,312
Maintenance & repairs		104,580	106,082	313,314
Other costs		24,534	43,426	105,180
Sub-total		170,940	362,954	678,805
Lost fuel gas costs (US$/y)				
Lost fuel gas	$5.55/GJ	905,024	1,141,305	1,322,605
Economics (US$/y)				
Capital expenditure		370,380	375,700	1,109,633
Operating expenditure		170,940	362,954	678,805
Lost fuel gas		905,024	1,141,305	1,322,605
Total		1,446,345	1,879,960	3,111,044

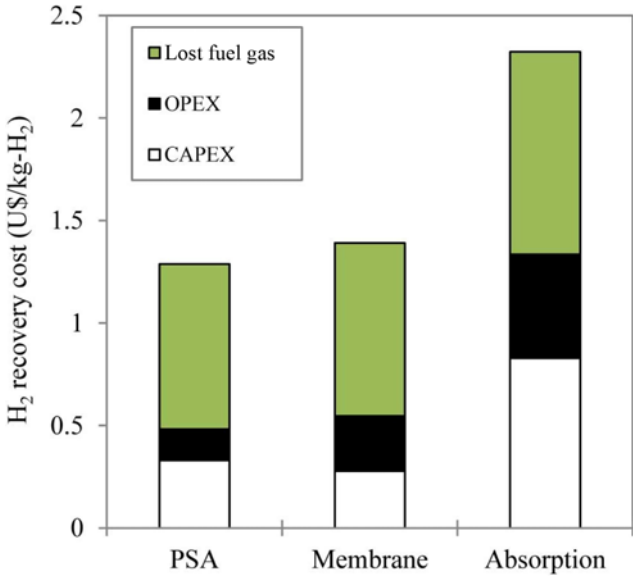

Fig. 18. Economics of hydrogen recovery from Tehran refinery off-gas.

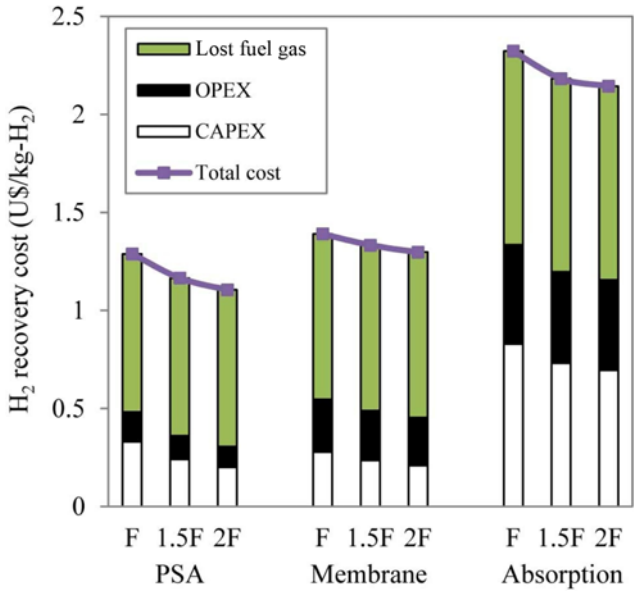

Fig. 19. Sensitivity analysis of feed flow rate on economics of the processes (F=115.99 kmol/h).

value was 0.51 when the flow rate was increased to 2F. This means that by increasing the feed flow rate, the PSA process became more economical.

Also, a sensitivity analysis of interest rate on the economics of the processes is shown in Fig. 20. As can be observed, reducing interest rate decreased cost of hydrogen recovery for all processes. But this reduced cost in the gas absorption process was highest in comparison to the other two processes.

For a better comparison between membrane and PSA processes, a membrane process with hydrogen recovery of 0.789 was considered in the economic comparison, which resulted in hydrogen purity of 0.995 (stage cut of 0.57). In this case, the total cost of the membrane process was U$ 1.40/kg-H_2. It should be noted that decreasing recovery of membrane process from 0.95 to 0.789 decreased the total cost of the membrane process from U$ 1,879,960 to U$ 1,573,052, but this value slightly increased from U$ 1.39 to U$ 1.40 per 1 kg recovered hydrogen. Accordingly, using the membrane process with lower recovery (or stage cut) can't be efficient and beneficial.

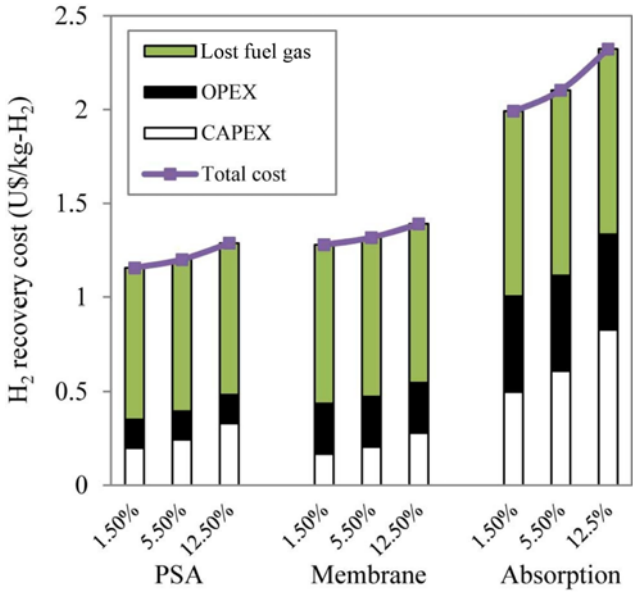

Fig. 20. Sensitivity analysis of interest rate on economics of the processes.

CONCLUSION

Simulation of hydrogen recovery process using the PSA is performed with 1.75 m×π m^2 silica gel adsorbent, for removing heavy compounds and 3.75 m×π m^2 activated carbon adsorbent for the removal of other impurities. It was observed with reducing feed pressure, the product purity reduced, but the recovery increased. Also, the purity profile of hydrogen illustrated that the bed becomes saturated after 7 minutes. So, if the absorption process lasts more than 7 minutes hydrogen purity in product drops.

Simulation of hydrogen recovery process was performed using one-stage polyimide membrane with an area of 334 m^2 to achieve stage cut of 0.7. With moving along the membrane length, the hydrogen purity in permeate side was slightly reduced, as a result of considerable hydrogen purity reduction in retentate side. By increasing pressure ratio, the product recovery and purity were increased. Increasing membrane area increased hydrogen recovery and decreased its purity.

To achieve high purity and recovery in gas absorption process, it is needed to do this process under temperature below 0 °C. It was observed that the purity and recovery were increased by decreasing absorption temperature. Also, by increasing the solvent flow rate and absorption pressure, purity was increased but recovery was reduced.

Finally, to determine a cost-effective process, the PSA, the gas absorption, and the membrane, processes were compared economically. The total cost of the PSA process was lower than the other processes, so using this process is advisable. On the other hand, the amount of recovered hydrogen in PSA process was lower than in membrane and gas absorption processes. If higher hydrogen recovery than the PSA recovery is required, the membrane process is economically more efficient in comparison to gas absorption process.

NOMENCLATURE

A_S : membrane area for each segment [m^2]
b_{0i} : Langmuir isotherm parameter [bar^{-1}]
F_F : feed flow rate [kmol/h]
F_P : permeate flow rate [kmol/h]
F_P^k : permeate flow rate leaving segment k [kmol/h]
$F_{P,l}^k$: local permeate flow rate passing through membrane at segment k [kmol/h]
F_R : retentate flow rate [kmol/h]
F_R^k : retentate flow rate leaving segment k [kmol/h]
L : membrane length [m]
m : number of components
P_P : pressure of permeate side [bar]
P_R : pressure of retentate side [bar]
P_F : feed pressure [bar]
P_i : partial pressure of component i [bar]
Q_i : permeance of component i [kmol m^{-2} h^{-1} bar^{-1}]
q_i : equilibrium loading of component i [mmol g^{-1}]
q_m : Langmuir isotherm parameter [mmol g^{-1}]
T : temperature [k]
x_i : mole fraction of component i in retentate
x_i^k : retentate mole fraction of component i leaving segment k
x_i^0 : mole fraction of component i in feed
y_i : mole fraction of component i in permeate
y_i^k : permeate mole fraction of component i leaving segment k
$y_{i,l}^k$: local permeate mole fraction of component i passing through membrane at segment k
z : axial distance [m]
$(-\Delta H_{Ai})$: heat of adsorption of component i [Jmol^{-1}]
†: 1 GPU=10^{-6} cm^3 (STP)/cm^2·s·cmHg

REFERENCES

1. R. Ramachandran and R. K. Menon, *Int. J. Hydrog. Energy*, **23**, 593 (1998).
2. N. Hallale and F. Liu, *Adv. Environ. Res.*, **6**, 81 (2001).
3. M. R. Sardashti Birjandi and F. Shahraki, *Chem. Eng. Technol.*, **34**, 1974 (2011).
4. P. Bernardo and E. Drioli, *Petroleum Chemistry*, **50**, 271 (2010).
5. A. Fonseca, V. Sá, H. Bento, M. L. C. Tavares, G Pinto and L. A. C. N. Gomes, *J. Cleaner Production*, **16**, 1755 (2008).
6. M. Mapiour, V. Sundaramurthy, A. K. Dalai and J. Adjaye, *Energy & Fuels*, **23**, 2129 (2009).
7. Y. R. Mehra and A. H. Al-Abdulal, Hydrogen Purification in Hydroprocessing, 103rd NPRA Annual Meeting, San Francisco, California USA, March 13-15 (2005).
8. S. Peramanu, B. G Cox and B. B. Pruden, *Int. J. Hydrog. Energy*, **24**, 405 (1999).
9. A. A. Al-Rabiah, Membrane Technology for Hydrogen Separation in Ethylene Plants, 4th Ibero-American Congress on Membrane Science and Technology (CITEM), Brazil, July 16-18 (2003).
10. S. P. Kaldis, G C. Kapantaidakis and G P. Sakellaropoulos, *J. Membr. Sci.*, **173**, 61 (2000).
11. A. Malek and S. Farooq, *AIChE J.*, **44**, 1985 (1998).
12. M. Yavary, H. Ale-Ebrahim and C. Falamaki, *Chem. Eng. Sci.*, **66**, 2587 (2011).
13. J. Yang, C.-H. Lee and J.-W. Chang, *Ind. Eng. Chem. Res.*, **36**, 2789 (1997).
14. R. W. Baker, *Ind. Eng. Chem. Res.*, **41**, 1393 (2002).

15. S. Peramanu, Absorption-Stripping Process for the Purification of High Pressure Hydrogen: Solubility, Mass Transfer and Simulation Studies, Ph.D. Dissertation, University of Calgary, Canada (1998).
16. A. Malek and S. Farooq, *AIChE J.*, **43**, 761 (1997).
17. K. Li, D. R. Acharya and R. Hughes, *J. Membr. Sci.*, **52**, 205 (1990).
18. S. Shokri, H. Ganji, M. Ahmadi Marvast and M. Bazmi, *Petroleum & Coal*, **50**, 1 (2008).
19. W. D. Seider and J. D. Seader, *Product and process design principles*, 2th Ed., John Wiley and Sons, Inc. (2004).